Chapter 6
Results and Analysis

6.1 General

The stability of the underground structures depends on the strength of the pillars and the behaviour of the overlying strata during depillaring operations. The stability of the pillars and the behaviour of the overlying strata was assessed in this study during depillaring operations. Numerical simulation techniques are used to simulate the model. The model comprises three panels, namely caved (A), working (B) and developed (C). A detailed analysis was carried out on strata issues during the depillaring operations in the working panel. It is of general understanding that the effect of the goaved-out panel will be on the adjacent panel. Therefore, a large model comprising three panels, A, B and C, was considered. The simulation results have been obtained in terms of stress acting on the pillars and displacement of overlying strata during depillaring operations.

6.2 Simulation results

The goaved-out panel A was simulated in one go using the explicit method of approach. The subsidence observed on panel A's dip and rise sides was about 1.52 m and 1.64 m, respectively. After simulating panel A, the results of the simulation, in terms of vertical stress on the standing pillars (including barrier pillars) in panels B and C, are shown in Fig. 6.1. The vertical stress patterns on the rise and dip sides of panel B are shown in Fig. 6.1b and 6.1c. The marked region in Fig. 6.1 highlights the unsymmetrical nature of the vertical stress due to the goaf effect, causing the goaf edge pillars to experience more vertical stress. Panel B consists of 85 pillars. The average vertical stress was calculated

by a FISH function, as shown in Fig. 6.2. The graphical representation in Fig. 6.2 shows that the goaf edge pillars experienced higher average vertical stress.

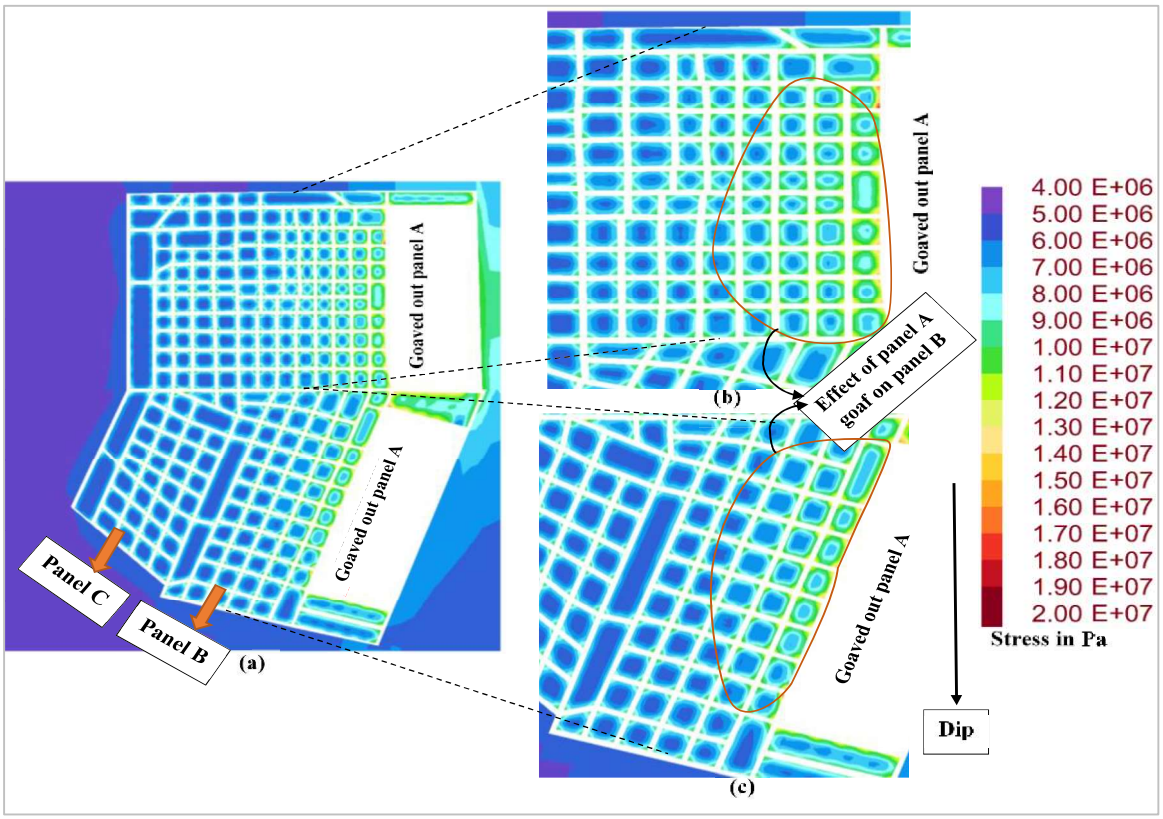

Figure 6.1: (a) Vertical stress profile on Panel B. (b). Magnified view of vertical stress profile on the rise side of panel B. (c) Magnified view of vertical stress profile on the dip side of panel B

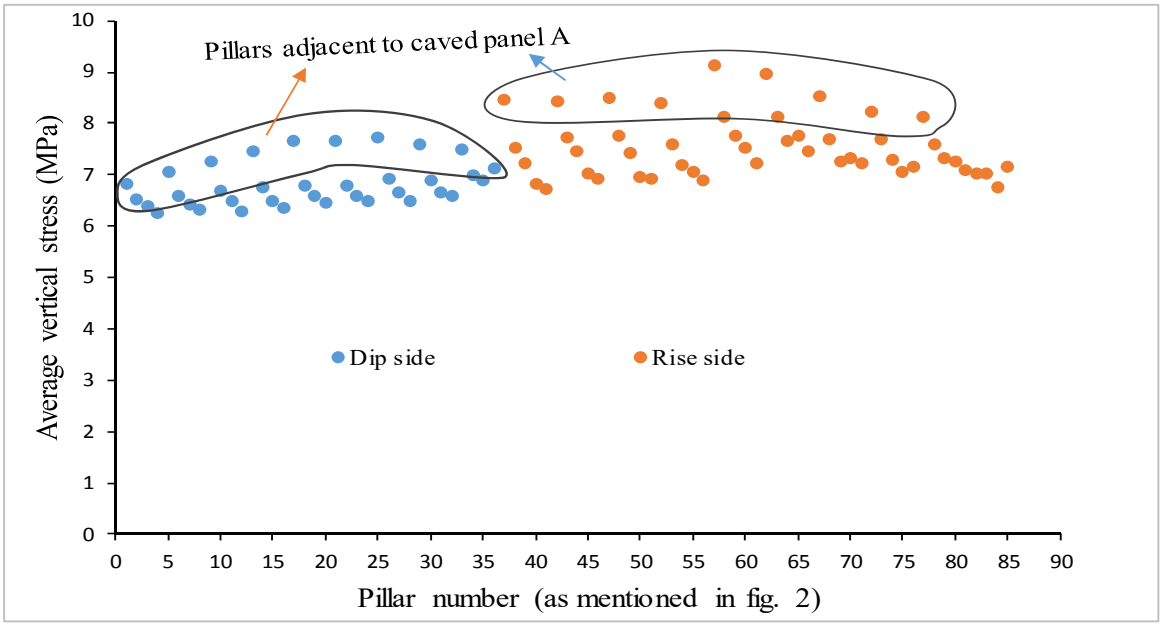

Figure 6.2: Average vertical stress on pillars during the development of panel B

During pillar-by-pillar extraction, the behaviour of the roof at different typical stages was presented in Fig. 6.3. The vertical stress profile on pillars before and after the first and second major falls were presented in Fig. 6.4. During depillaring operations with a goaf exposure of 9,782 m², a first local fall of 5 m was observed as shown in Fig. 6.3a. As depillaring continued, the roof strata above the goaf behaved like a hanging beam. The first major fall occurred after extracting 11 pillars over a goaf area of 14,853 m², resulting in a 35 m roof collapse as shown in Fig. 6.3c. Before this fall, the immediate roof acted like a cantilever beam with an overhang of about 0.4 m (Fig. 6.3b). Because of the cantilever beam, the goaf edge pillar (pillar 11) experienced a maximum induced stress of about 9.49 MPa, as shown in Fig. 6.4a. During the first major fall, the cantilever beam caved. As a result, the stress observed on the goaf edge pillar (pillar 12) was about 8.44 MPa, as shown in Fig. 6.4b. As the goaf area increased to 19,893 m², the strong overlying strata continued to overhang in the goaf as shown in Fig. 6.3d. A second major roof fall occurred at a goaf exposure of 21,087 m², with an overhang of 0.23 m as shown in Fig. 6.3e. Before the second major fall, the goaf edge pillar (pillar 15) experienced induced stress of about 10.24 MPa, and after the major fall, the stress dropped to 8.28 MPa, as shown in Fig. 6.4c and 6.4d. With further increase of goaf area to 26,161 m², a third major roof fall and delamination of layers were observed, leading to 0.17 m of subsidence as shown in Fig. 6.3f. Subsequent goaf line advancement to 31,505 m² resulted in 0.31 m of subsidence, and further extraction to 38,007 m² increased subsidence to 1.03 m. The complete extraction of panel B's dip side, consisting of 32 pillars, resulted in a surface subsidence of 1.28 m, as shown in Fig. 6.3h.

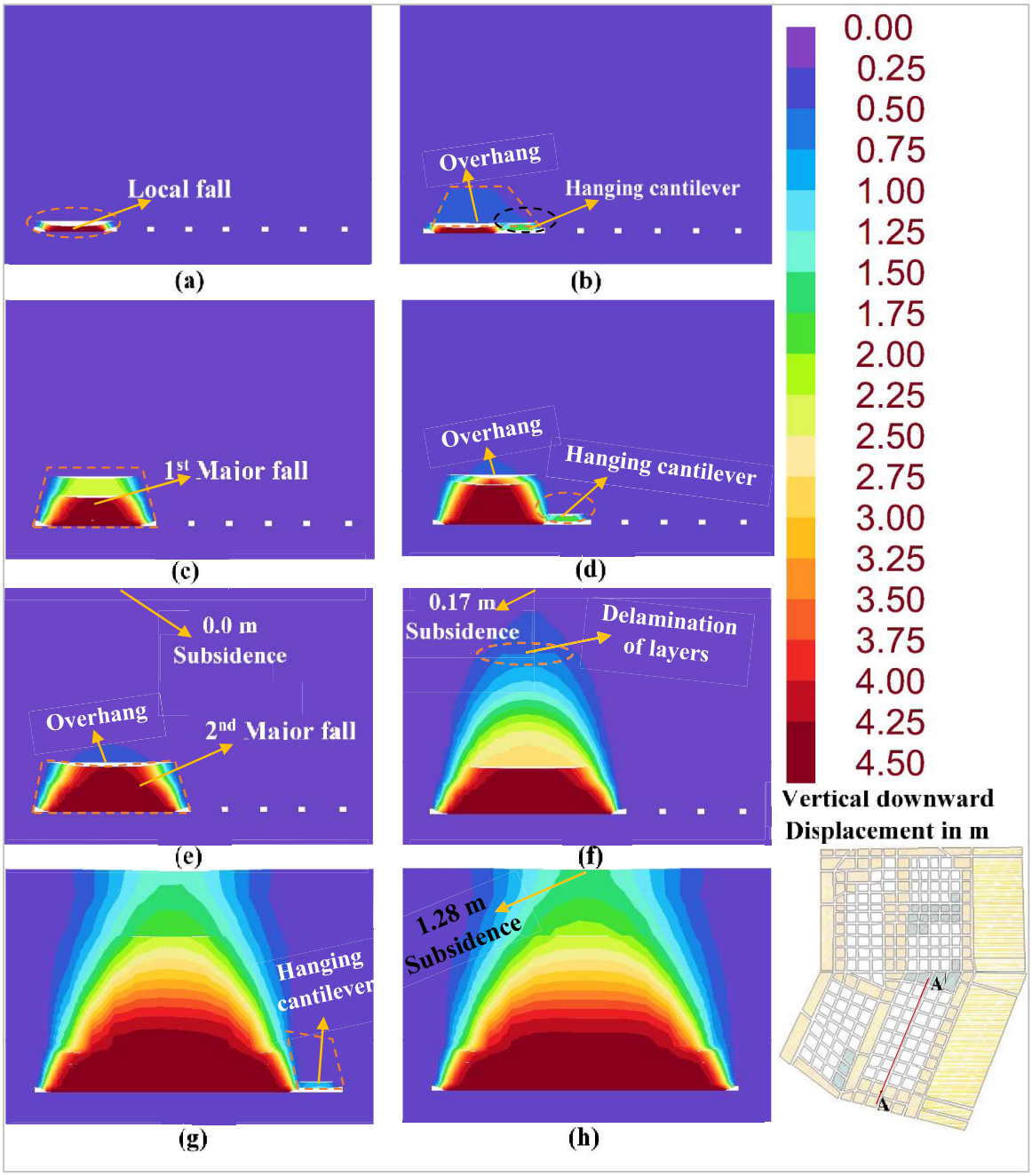

Figure 6.3: Vertical downward displacement of the strata in the dip side of panel B (along A-A^{I} section) with the advancement of goaf

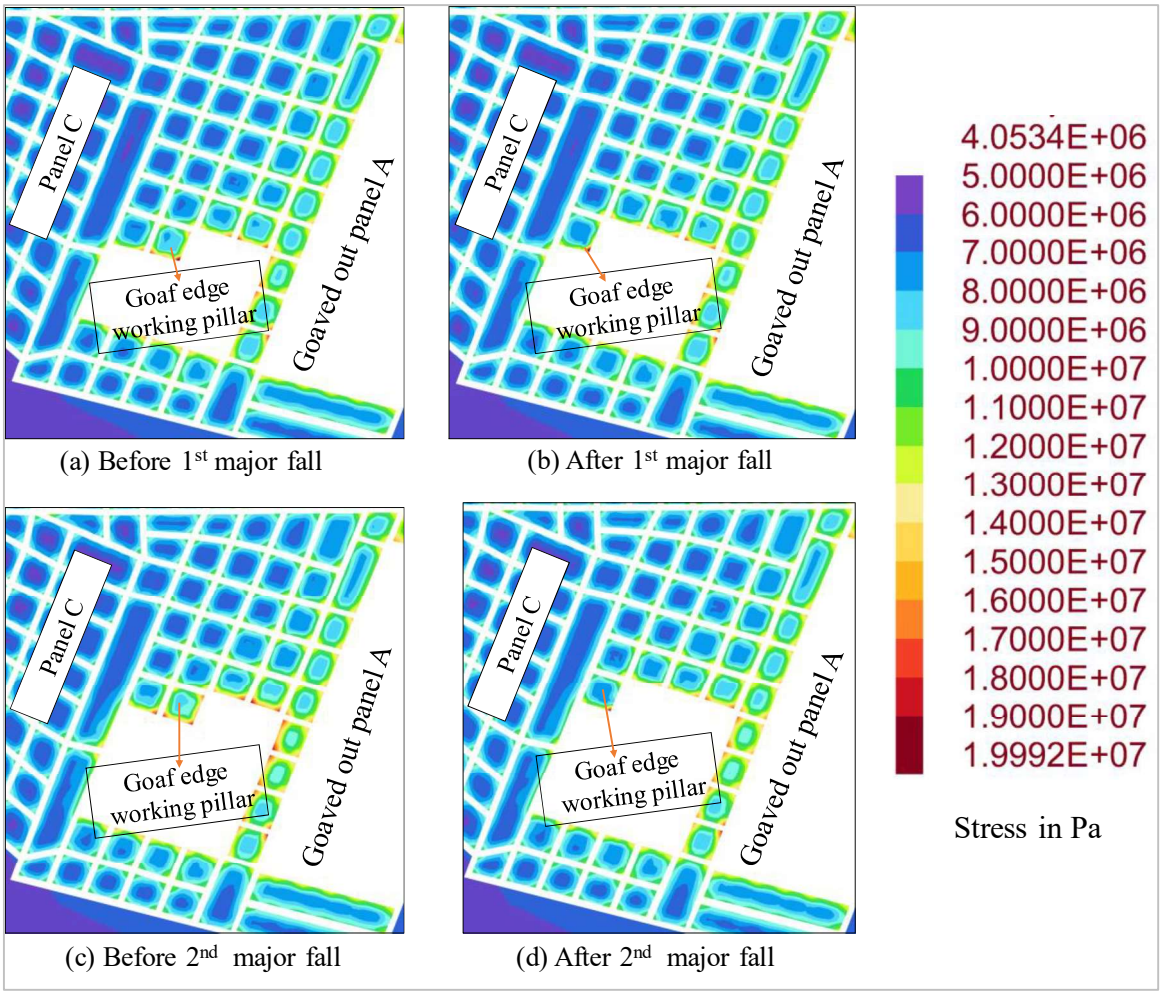

Figure 6.4: Magnified view of vertical stress profile on the dip side of panel B at various depillaring stages

During the advancement of the goaf line on the rise side of panel B, the first local fall was observed at a goaf area of 7,960 m², as shown in Fig. 6.5a. As the goaf area increased to 13,423 m², a major fall occurred, with a 35 m roof caving (Fig. 6.5c). Before the major fall, an overhang with a vertical displacement of about 0.24 m was observed in the main roof, which behaved like a cantilever beam (Fig. 6.5b). As a result of the overhang in the roof, the goaf edge pillar (pillar 49) experienced an average induced stress of about 11.54 MPa, as shown in Fig. 6.6a. After the major fall, there was a drop of vertical stress observed on the goaf edge pillar 50, resulting in an average vertical stress of about 10.49 MPa (Fig. 6.6b). During the pillar-by-pillar extraction on the rise side, some strata issues were observed after the extraction of pillar 54. As a result, pillars from 55 to 67 were left in the field. A similar scheme was considered in the simulation. Consequently, 13 pillars (55 to 67) were left in place, and depillaring resumed from pillar 68. Fig. 6.6c shows the stress profile on the pillars after extraction of pillar 54. After a goaf exposure of 8,381 m², a local fall was observed, and at a goaf area of 12,468 m², a major fall occurred (Fig. 6.5e and f). Before this major roof fall, an overhang of 0.41 m was observed in the roof (Fig. 6.5e). As a result, the goaf edge pillar (pillar 81) showed an average vertical stress of about 11.13 MPa, and after the major fall, the vertical stress observed on the goaf edge pillar (pillar 82) showed induced stress of about 10.1 MPa, as shown in Fig. 6.6d and e. On the rise side of panel B, the average vertical stress observed was about 11.57 MPa before the major fall on pillar 49.

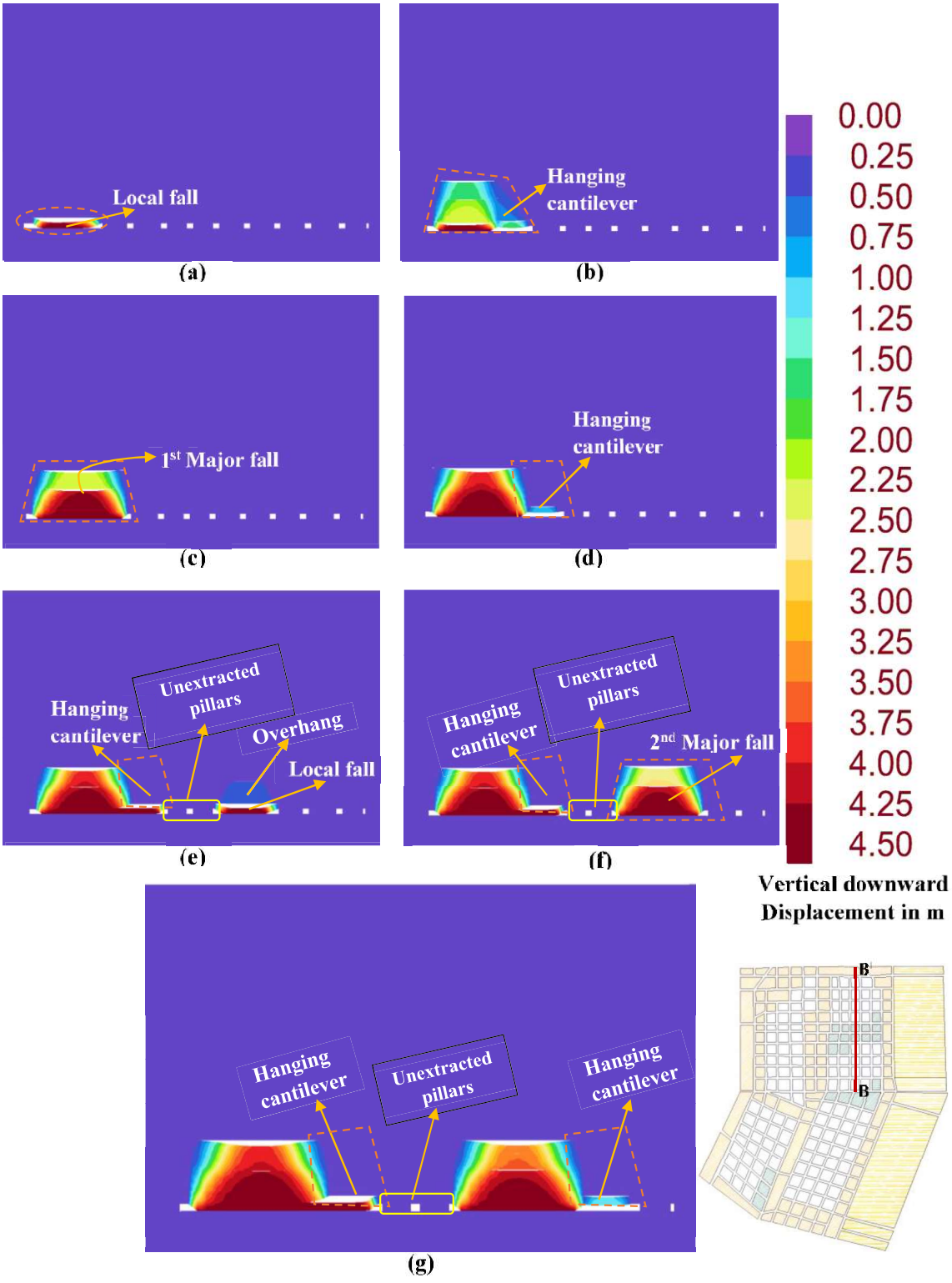

Figure 6.5: Vertical downward displacement of the strata in the rise side of panel B (along B-B^{I} section) with the advancement of goaf

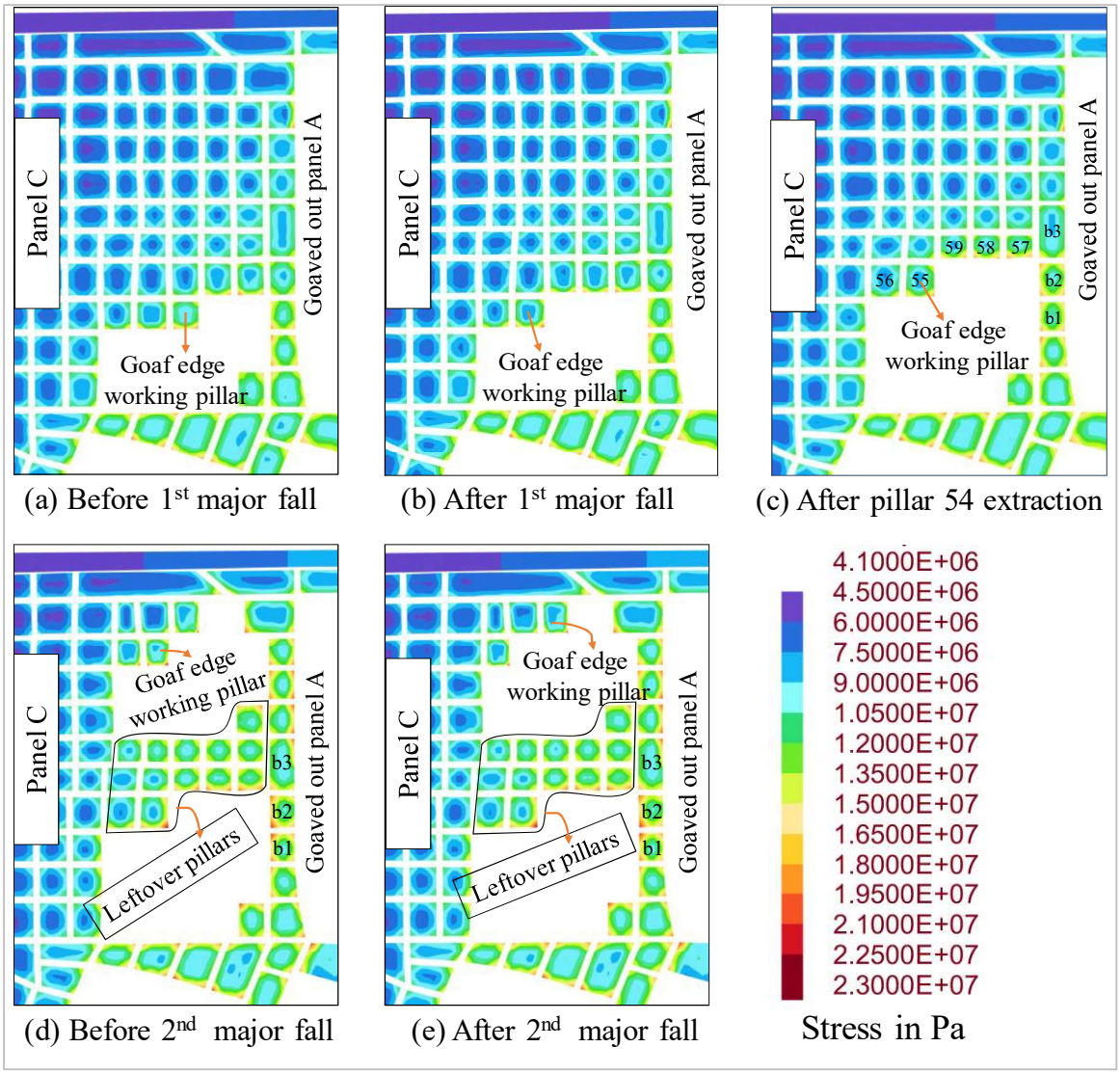

Figure 6.6: Magnified view of vertical stress profile on the rise side of panel B at various depillaring stages

6.3 Analysis

The effect of the goaf is clearly shown in Fig. 6.1 and 6.2. The influence of goaf in terms of vertical stress on pillars can also be calculated using the empirical equation suggested by Peng and Chiang (Peng and Chiang 1984). Estimated the extent of a zone carrying 100% of the load transferred distance from the goaf by using equation 6.1.

$$D_{1.0} = 9.3\sqrt{H} \quad \text{----------(6.1)}$$

Where "$D_{1.0}$ distance into the side abutment at which the stress resulting from mining is no longer detected, and H is the working depth (m)". The influence of goaf (LTD) from the simulation results and empirical equation (equation 6.1) were calculated and shown in Table 6.1. The simulation results show that the influence of caved panel A on the dip side of panel B was less compared to the rise side of panel B (Table 6.1).

Table 6.1: Load transferred distance from the gob in panel B

Depillaring panel B	LTD from equation 12 (m)	Approximate LTD from simulation results (m)
Dip side	131.5	109
Rise side	131.5	140

The stability of the pillars has been assessed by the FOS. The FOS was calculated for each working pillar (goaf edge pillar) during the sequential extraction. On the dip side, after the development stage, the FOS of the working pillars was observed to be between 1.7 and 2.4. The FOS on the rise side was also calculated. On the rise side of panel B, 13 pillars were left (pillars 55 to 67) because of strata issues in the field. The simulation results showed that six goaf edge pillars (including the barrier) had a FOS of less than 1.3 after the extraction of pillar 54. Table 5 shows the average vertical stress and FOS of goaf edge leftover pillars (pillar numbers 57, 58, and 59) and barrier pillars (b1 and b2) during development and after the extraction of pillar 54. The proposed time-dependent pillar strength equation (see equation 4.14) is used to calculate the pillar strength. Due to the low FOS and high-induced vertical stress observed on the rise side, the goaf edge's leftover pillars were critically analysed. The simulation results mentioned in Table 6.2 showed that the high abutment load on the barrier pillars (with FOS near 1.3) led to the yielding of these pillars. As a result of the yielding barrier pillars, the vertical load of panel A was transferred to panel B's working area, making the effect of the goaf more

apparent on the rise side than on the dip side of panel B. The influence of goaf on the rise side was greater than the dip side mainly because of the yielding of the barrier pillars. As a result, the load transfer distance was more on the dip side than the rise side, as shown in Table 6.1. Consequently, the working pillars in that region experienced higher vertical stress. From the simulation results, it was anticipated that the failure of the barrier pillar could be the main reason for significant strata issues during the extraction of pillar number 54 in the field.

Table 6.2: Average vertical stress and FOS of leftover and rib pillars on the rise side of panel B after extraction of pillar 54

Pillar number	Strength (MPa)	Development stage		Depillaring stage	
		Average vertical stress (MPa)	FOS	Average vertical stress (MPa)	FOS
57	14.07	8.85	1.59	12.25	1.15
58	14.23	8.17	1.74	12.06	1.18
59	14.16	7.82	1.81	11.2	1.26
b1	14.87	9.78	1.52	12.93	1.15
b2	15.25	9.68	1.58	13.03	1.17

6.4 Design of mechanised depillaring panel

Based on the analysis of panel B, panel C was modified to prevent similar strata issues. The next panel C, consists of 78 pillars, with 28 pillars on the dip side and 50 pillars on the rise side of the panel. As panel B faced strata issues on the rise side and because of the small size of the pillars, two rows of barrier pillars were suggested to be left against the goaf in panel C. The panel width was also reduced to 3 rows of pillars on the rise side. On the dip side, three pillars (pillars 1, 5, and 9) were left due to other strata issues. Fig. 6.7 shows the modified design layout of panel C after the completion of panel B. The numbering in Fig. 6.7 shows the line of extraction of panel C. The modelling results

showed that before starting the depillaring operations in panel C, the subsidence over panel A was about 1.57 m on the rise side and 1.7 m on the dip side, while the subsidence on the dip side of panel B was about 1.28 m.

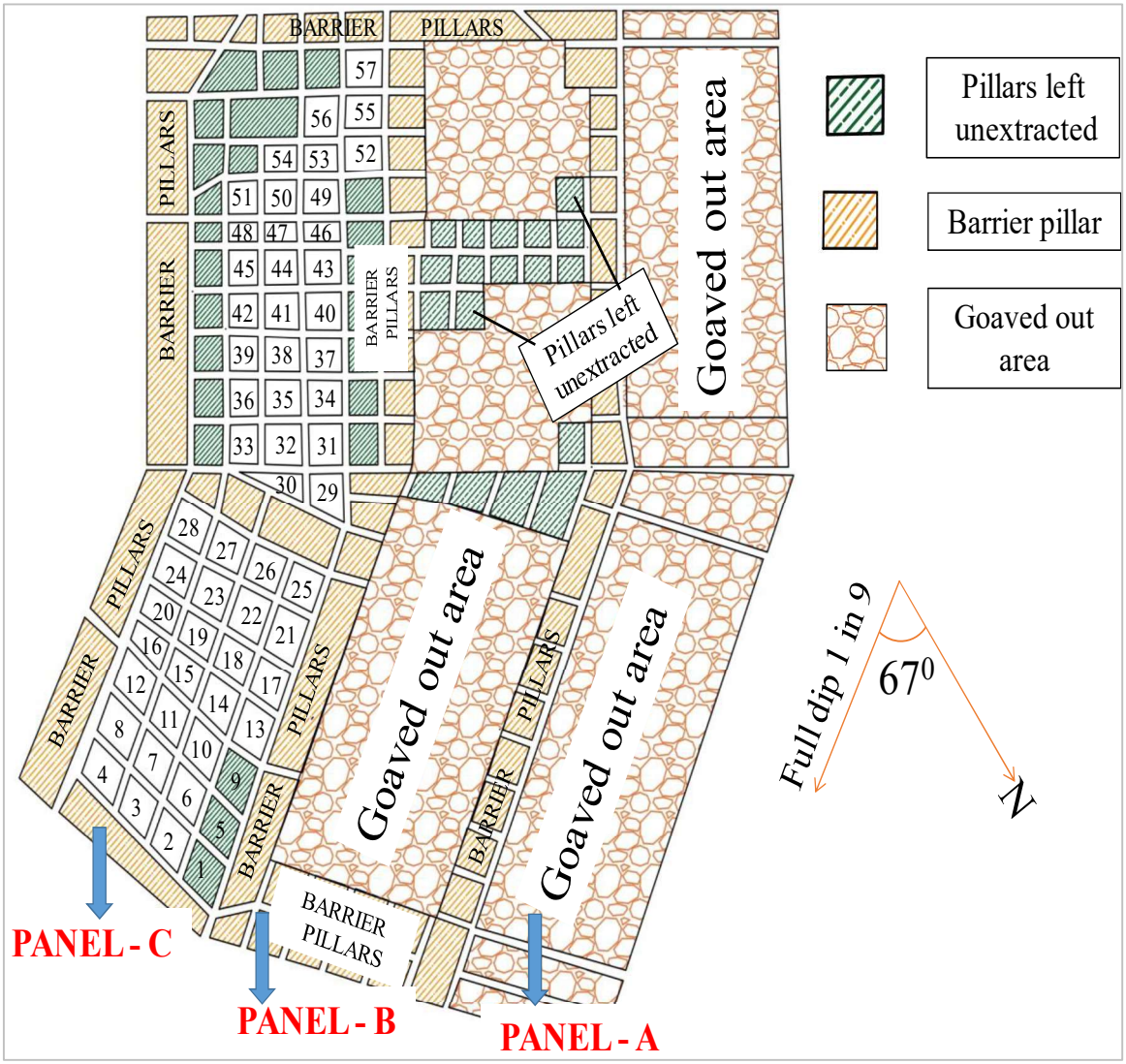

Figure 6.7: Modified layout of panel C along with goaved out panels A and B

6.4.1 Numerical Simulation of Panel C

After the complete extraction of panel, A, followed by panel B, the vertical stress acting on the developed pillars in panel C is shown in Fig. 6.8a (Figs. 6.8b and c show the vertical stress patterns on the rise side and dip side of panel C, respectively). The results showed that on the dip side of panel C, the effect of the goaf from panel B was observed up to the single-column pillars. On the rise side, it was observed within the barrier pillar region,

mainly because of leaving two rows of pillars. The effect gradually decreased, such that the last column pillars showed less vertical stress. Fig. 6.9 shows the graphical representation of vertical stress during the development stage in panel C. The marked pillars in Fig. 6.9 are the goaf edge pillars on the dip side, which show more average vertical stress

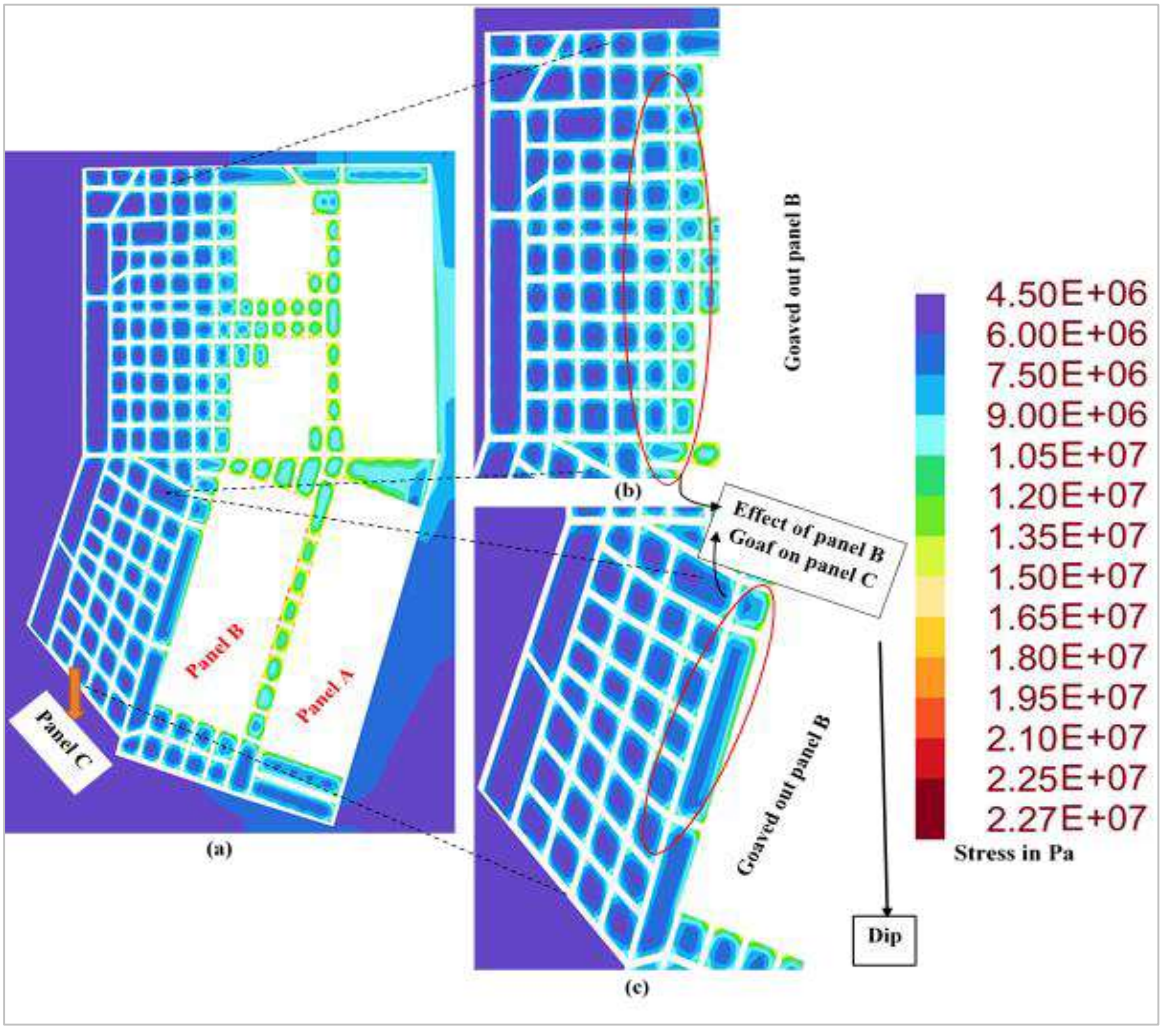

Figure 6.8: (a)Vertical stress profile on Panel C. (b). Magnified view of vertical stress profile on the rise side. (c) Magnified view of vertical stress profile on the dip side of the panel C

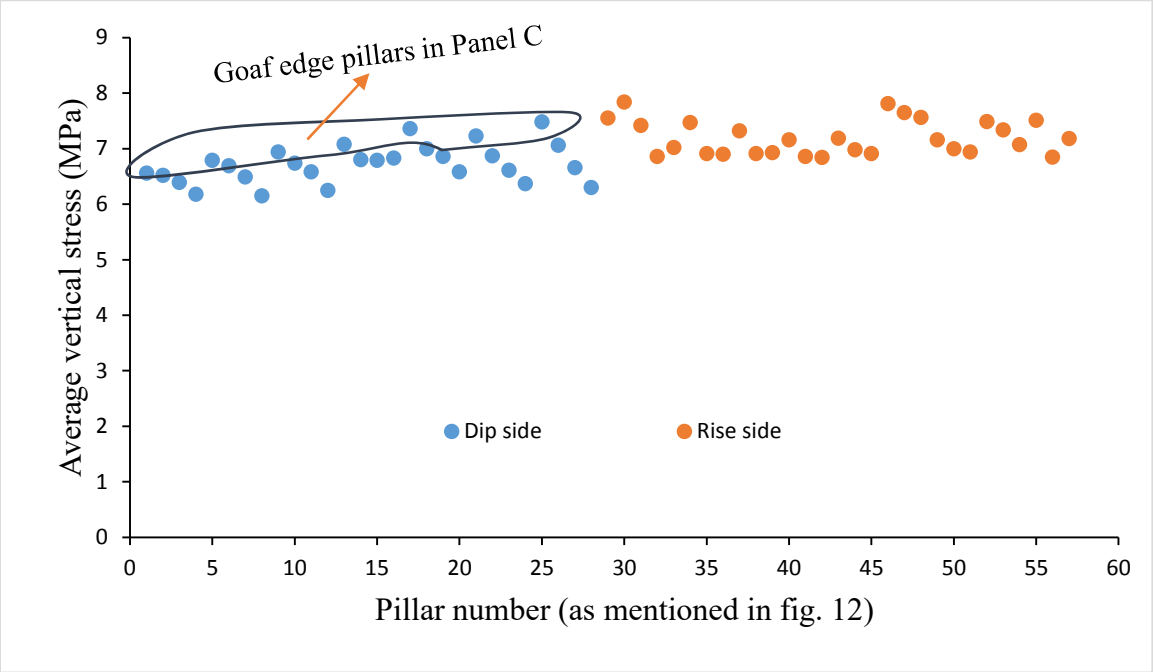

Figure 6.9: Average vertical stress on pillars during the development of panel C

During the pillar-by-pillar extraction in panel C, the caving behaviour and induced stress on the pillars were closely monitored. Fig.6.10 illustrates the vertical stress profile on pillars, and Fig. 6 .11 shows the displacement of overlying strata on the dip side of panel C. With the advancement of the goaf line, the first local fall occurred after extracting six pillars, resulting in a goaf area of 8,616 m^2. During this event, a 5 m thick immediate roof bed caved, as depicted in Fig. 6.11a. Subsequently, with increasing goaf area to 15,470 m^2, a first major fall was observed, involving a 35 m roof collapse above the immediate roof, shown in Fig. 6.11b. Before the first major fall, the goaf edge working pillar (pillar number 9) experienced average vertical stress of about 9.29 MPa (Fig. 6.10a). After the major fall, the stress observed on the goaf edge working pillar dropped to about 8.45 MPa as shown in Fig. 6.10b. With further advancement of the goaf, a second major fall occurred over a goaf exposure of 23,463 m^2. An overhang of 0.43 m was observed in the overlying strata, as seen in Fig. 6.11d. Prior to this second major fall, a hanging cantilever was observed at a goaf exposure of 21,828 m^2, as illustrated in Fig. 6.11c. Because of the hanging cantilever before the second major fall, the average vertical stress

on the goaf edge working pillar rose to about 10.51 MPa, and after the fall, it decreased to about 9.78 MPa as shown in Fig. 6.10c and d. Further extraction of pillars led to progressive goaf advancement, with observations of delamination of layers in the roof after a goaf exposure of 27,162 m^2. This delamination initially indicated a subsidence of approximately 0.1 m on the surface, as shown in Fig. 6.11e. As the goaf area increased to 29,616 m^2, the subsidence increased to 0.4 m. Finally, after the complete extraction of the dip portion (area of 32,036 m^2) of panel C, a subsidence of 1.03 m was observed on the surface, as depicted in Fig. 6.11f. The simulation results revealed that after each major fall, there was a significant reduction in vertical stress on the goaf edge pillars (0.84 MPa during the first major fall and 0.73 MPa during the second major fall).

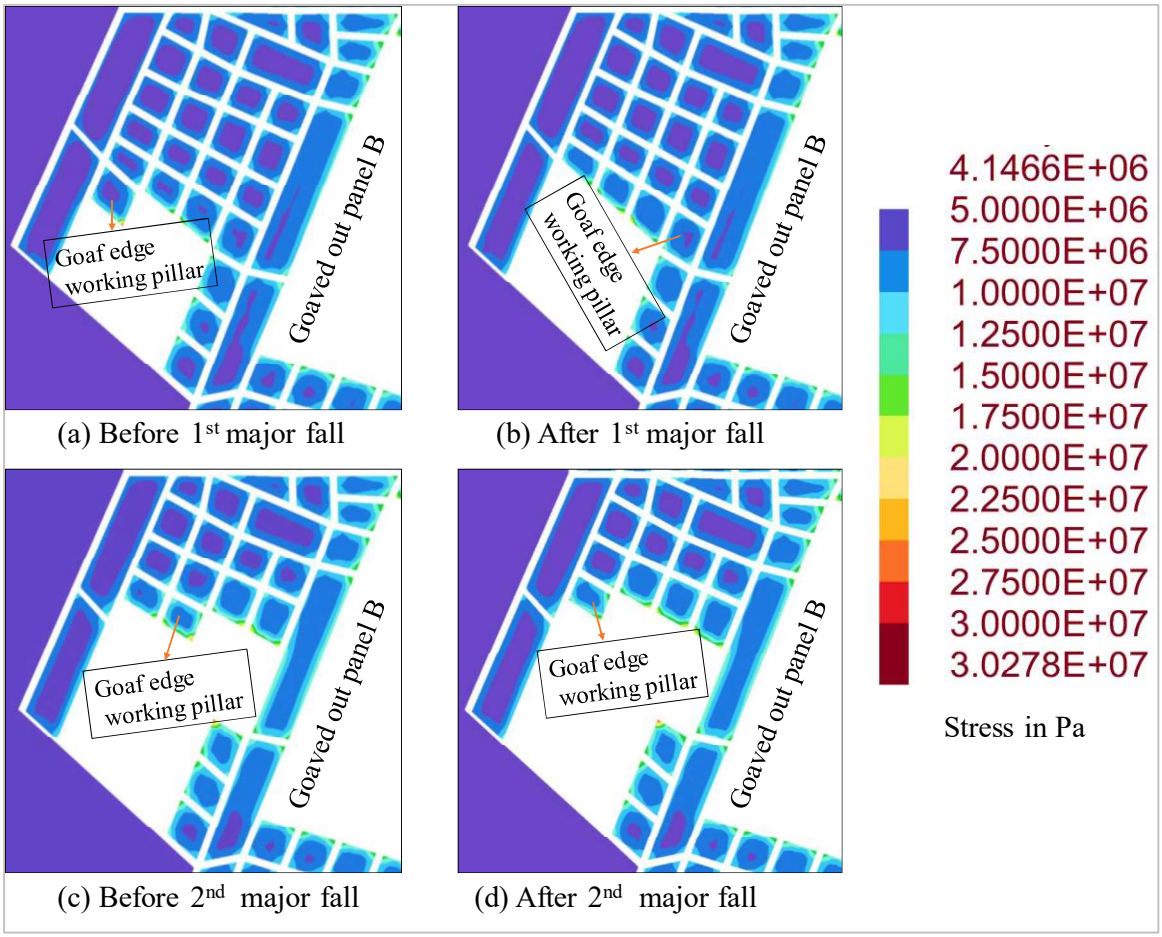

Figure 6.10: Magnified view of vertical stress profile on the dip side of panel C at various depillaring stages

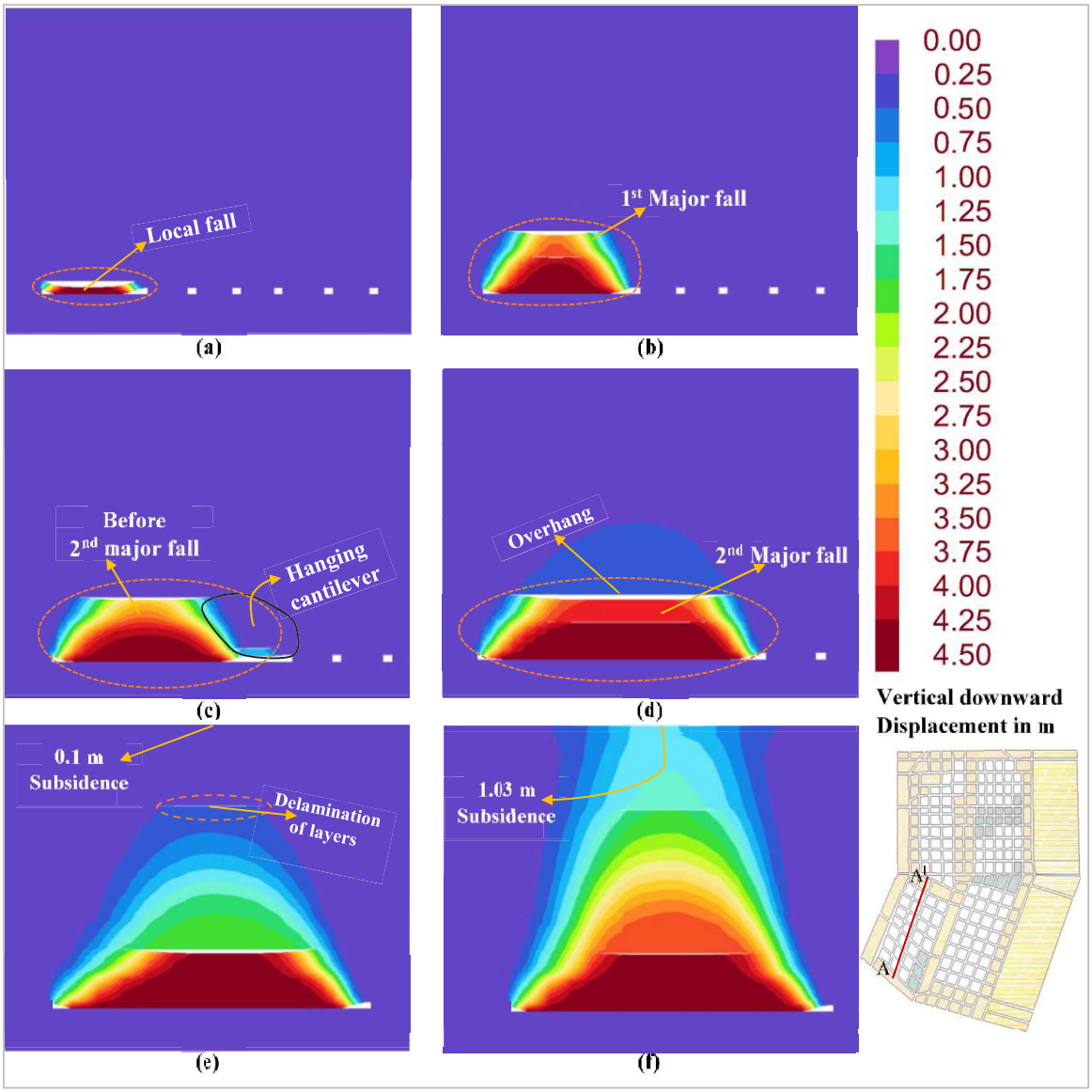

Figure 6.11: Vertical downward displacement of the strata in the dip side of panel C (along A-A^{l} section) with the advancement of goaf

On the rise side of panel C, two rows of barrier pillars were left; because of this, the goaf effect of panel B was much less. On the rise side of panel C, significant roof falls were observed during the advancement of the goaf line starting from pillar number 29. Five roof falls (including local and major falls) were observed. The first local fall occurred after a goaf exposure of 6,678 m², as illustrated in Fig. 6.12a. Subsequently, as the goaf area increased to 11,288 m², the first major fall was observed, depicted in Fig. 6.12c. Prior to this major fall, an overhang of 0.3 m was observed in the overlying strata, as shown in Fig. 6.12b. Because of the overhang before the first major fall, the average induced vertical stress on the goaf edge working pillar was about 9.61 MPa, and after the fall, it decreased to 9.33 MPa, as shown in Fig. 6.13a and b. As the goaf area further expanded to 17,969 m², a second major fall occurred with an overhang of 0.1 m, shown in Fig. 6.12d. Before the second major fall, the goaf edge pillar (pillar 39) experienced an average induced stress of about 9.82 MPa (Fig. 6.13c). After the major fall, the stress decreased to 9.13 MPa, as shown in Fig. 6.13d. The third major fall was observed with further advancement of the goaf area to 24,997 m², where the overlying strata above the caved rock behaved like a hanging beam with a vertical displacement of 0.6 m, as depicted in Fig. 6.12e. During the sequential extraction, a first indication of subsidence, approximately 0.13 m, was observed at a goaf exposure of 28,318 m². Following the complete extraction of the rise portion of panel C (goaf area of 32,207 m²), a subsidence of 0.38 m was observed on the surface, shown in Fig. 6.12f. During depillaring operations, pillars 46, 47 and 48 experienced maximum average vertical stress of about 11.49 MPa, 12.44 MPa and 11.22 MPa, respectively.

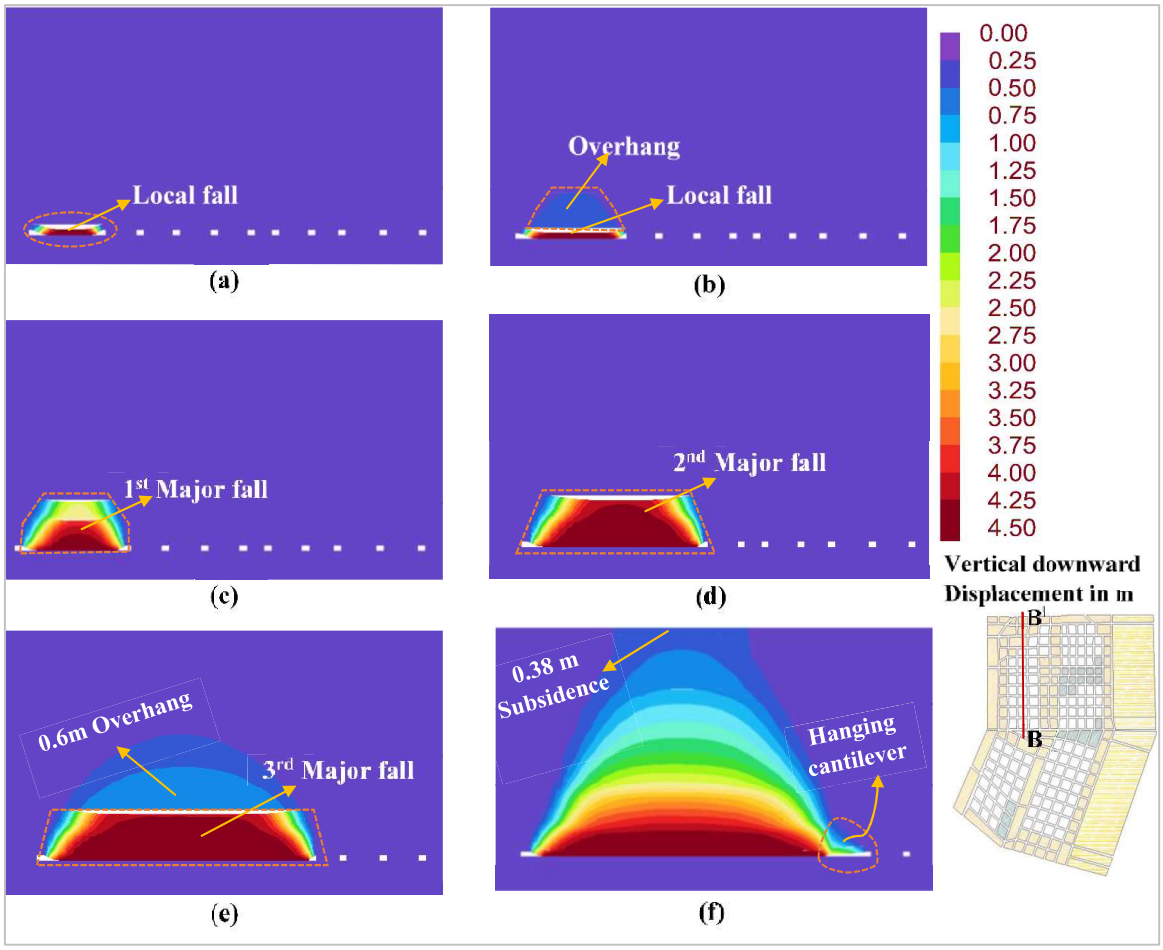

Figure 6.12: Vertical downward displacement of the strata in the rise side of panel C (along B-B^{I} section) with the advancement of goaf

Figure 6.13: Magnified view of vertical stress profile on the rise side of panel C at various depillaring stages

During the development stage, the minimum Factor of Safety (FOS) observed on the dip side of panel C was about 2.15, and on the rise side, it was approximately 1.6. During depillaring operations, except for pillars 46, 47, and 48, all pillars on panel C's dip and rise sides exhibited an FOS above 1.3. The lower FOS values were attributed to the smaller size of the pillars. Based on the FOS values obtained from simulation results, it was observed that pillars showed stable behaviour during depillaring in panel C, and no significant strata issues were observed. This favourable outcome was largely attributed to the proposed design approach, which included the strategic placement of barrier pillars. The proposed approach was successfully implemented in the field and extracted without strata issues. A partial extraction was suggested for pillars (46, 47, and 48) with an FOS of about 1.3 to minimise the strata issues.

6.5 Validation of the simulation results

The vertical displacement during the depillaring operations has also been monitored after the extraction of goaved-out panel A. The modelling results show that the maximum subsidence on the dip and rise sides of panel A was about 1.52 m and 1.64 m, respectively. These values slightly increased after the extraction of the next panels. This increase in subsidence was mainly due to the consolidation of roof strata over time. Similarly, the subsidence after extraction of panels B and C by numerical simulation techniques was monitored. The vertical displacement of strata along section C-C$^{|}$ after complete extraction of all the selected three panels is shown in Fig. 6.14. The displacement contours on the surface after extraction of all the panels is shown in Fig. 6.15. The subsidence in the field is also monitored in a grid pattern. These data have been interpolated to get the subsidence along the C-C$^{|}$ section. Fig. 6.16 shows the comparison of the subsidence profile from

numerical results with field measurements (along section C-C^{l} as shown in Fig. 6.15). The orange colour subsidence profile shows the results obtained from numerical simulation results, and the blue colour subsidence profile shows the subsidence profile obtained from field measurements. From the Fig. 6.16, it was observed that at the middle of each panel (i.e. Panel A, B and C), the subsidence obtained from simulation results is more compared with the subsidence measured from the field. After the extraction of panels, A, B and C, the subsidence observed in the field was about 1.2 m, 1.16 m and 0.79 m, respectively. The simulation results showed that the subsidence observed after the complete extraction of panels A, B, and C was 1.59 m, 1.3 m, and 1.03 m, respectively. The modelling results showed higher values in terms of subsidence because complete extraction was considered in the modelling.

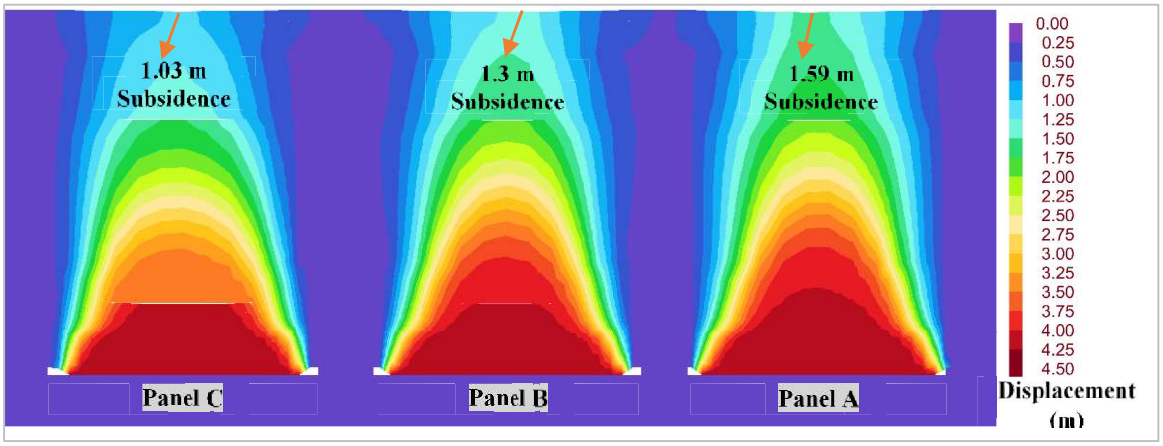

Figure 6.14: Displacement of overlying strata after complete extraction of panels A, B and C (along section C-C^{l} as shown in Fig 6.15)

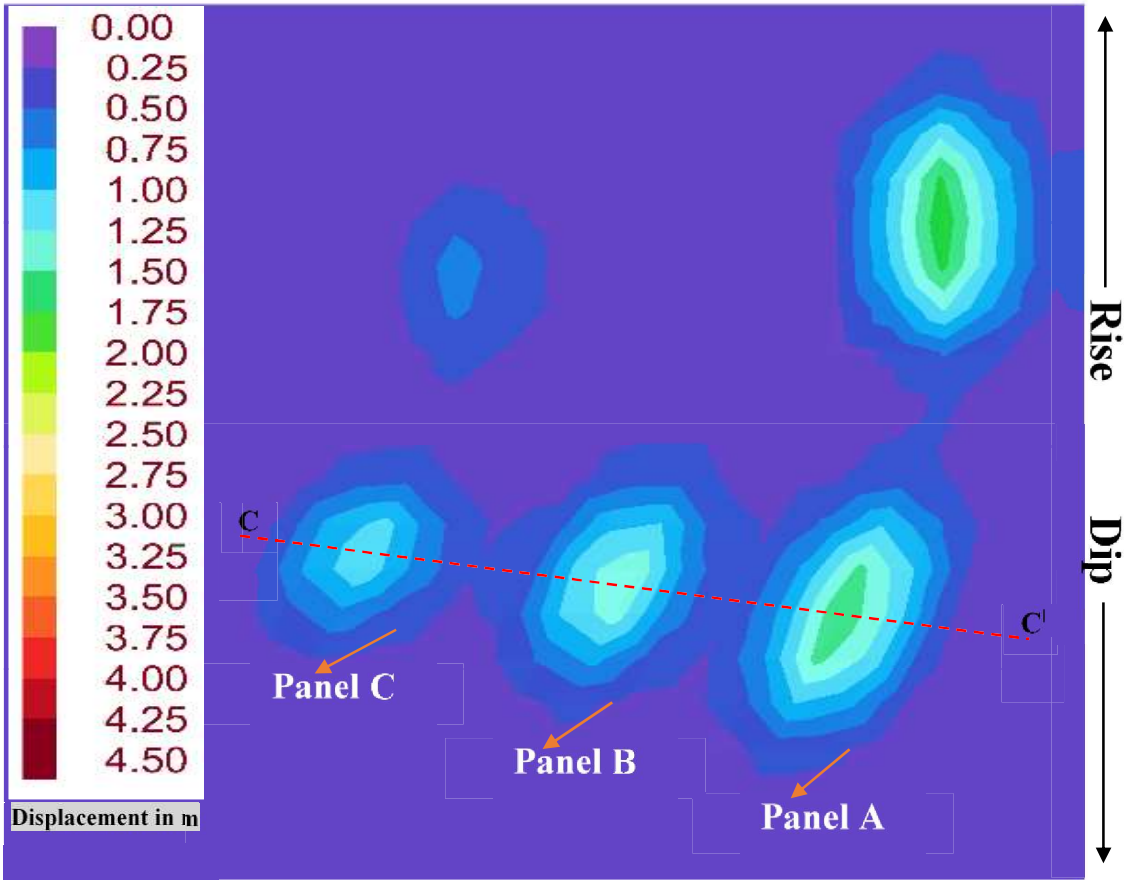

Figure 6.15: Displacement contour on the surface after complete extraction of panels A, B and C

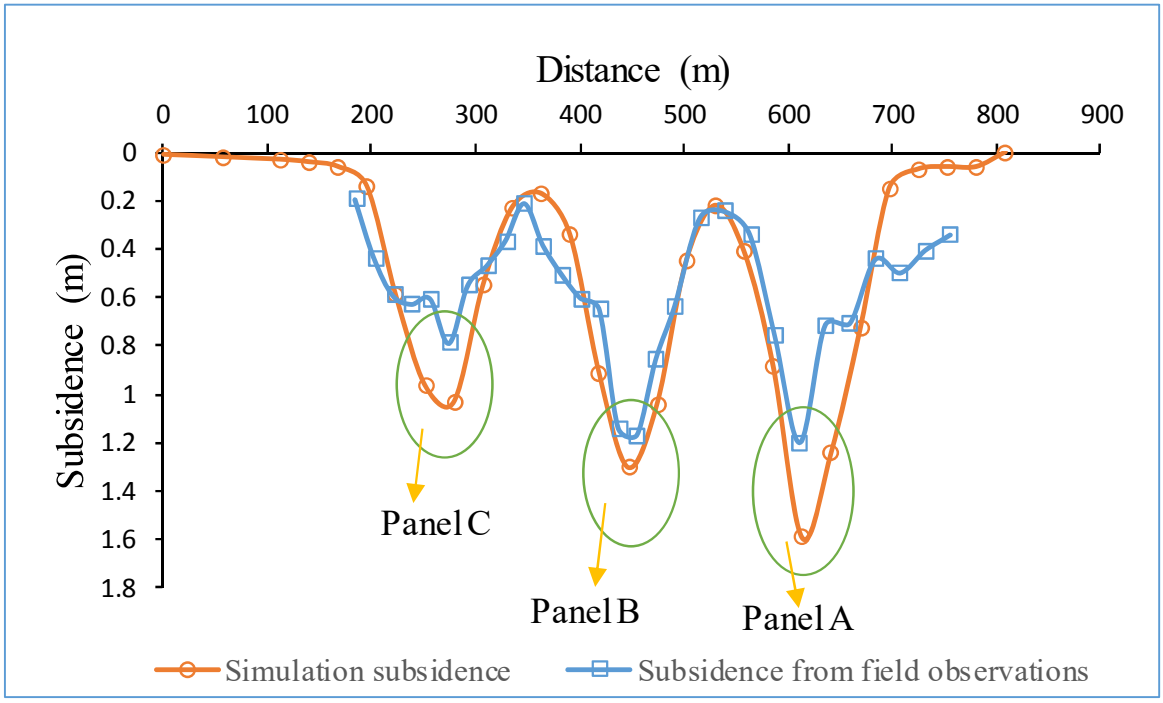

Figure 6.16: Comparison of subsidence profile from numerical results with field measurements (along section C-C')

During the extraction of pillar number 54 on the rise side of panel B, strata issues were observed with up to two rows of pillars. Simulation results show that the factor of safety (FOS) of goaf edge pillars (pillars 57, 58, and 59) and barrier pillars (b1, b2, and b3) was near 1.3 (as shown in Table 6.2). Because of the lower FOS values observed on the barrier pillars (b1, b2, and b3), the load of panel A was transferred into the working area of panel B, causing the pillars in that region to experience more induced stress. Consequently, the working pillars also showed lower FOS values. These lower FOS values of the pillars created unstable working conditions in the field. Field observations showed that in panel B and panel C, the first major roof fall was observed after the goaf exposure of about 13,008 m² and 17,021 m², respectively. The simulation results indicated that with the progressive advancement of the goaf, the first major roof fall occurred after a goaf area of 14,853 m² in panel B and 15,470 m² in panel C. The study validates its simulation results regarding subsidence observed on the surface, strata issues observed on the rise side of panel B, and the first major roof fall area during depillaring operations in panels B and C.

6.6 Concluding remarks

The proposed explicit caving simulation approach has been considered to assess the caving behaviour and the status of the pillars of a depillaring mine. A case study of a depillaring mine with three panels (A, B, and C) was considered. The simulation results showed that during depillaring on the dip side of panel B, the FOS of the working pillars was estimated to be more than 1.7. However, on the rise side of panel C, some of the goaf edge pillars, including barrier pillars, had a FOS in the range of 1.3 to 2.5, leading to excessive side spalling of pillars. A similar situation was also observed in the field. In situations where the FOS of the barrier pillars is less than 1.3, it is not feasible to increase the barrier size. Therefore, reducing the panel size and leaving an extra row of barrier

pillars is the only option for ensuring panel stability. Based on this analysis, it was suggested that the minimum FOS of the working pillars should be more than 1.3, preferably 1.5, as a design criterion for the panel. Using this criterion, the next panel layout was proposed and numerically simulated to ensure it met the design requirements. The proposed panel was then investigated during the depillaring operations, where no major strata-related issues were observed. The field observations, including the area of the first major fall and the subsidence profile, were largely in agreement with the numerical simulation results.